Li, X., Tan, H., Li, X., Dick, G., Wickert, J., Schuh, H. (2018): Real-Time Sensing of Precipitable Water Vapor From BeiDou Observations: Hong Kong and CMONOC Networks. - *Journal of Geophysical Research*, *123*, 15, pp. 7897—7909.

DOI: http://doi.org/10.1029/2018JD028320

Journal of Geophysical Research: Atmospheres

RESEARCH ARTICLE
10.1029/2018JD028320

Real-Time Sensing of Precipitable Water Vapor From BeiDou Observations: Hong Kong and CMONOC Networks

Xingxing Li[1,2], Han Tan[1], Xin Li[1], Galina Dick[2], Jens Wickert[2], and Harald Schuh[2]

[1]School of Geodesy and Geomatics, Wuhan University, Wuhan, China, [2]GFZ German Research Centre for Geosciences, Potsdam, Germany

Key Points:
- Precipitable water vapor was retrieved based on the real-time precise point positioning ambiguity resolution approach
- Real-time PWV acquired using the BDS fixed solution was more accurate and reliable than that with BDS float solution
- Real-time PWV retrieved from the BDS observations can contribute to time-critical meteorological applications

Correspondence to:
X. Li,
lixinsgg@whu.edu.cn

Citation:
Li, X., Tan, H., Li, X., Dick, G., Wickert, J., & Schuh, H. (2018). Real-time sensing of precipitable water vapor from BeiDou observations: Hong Kong and CMONOC networks. *Journal of Geophysical Research: Atmospheres*, *123*, 7897–7909. https://doi.org/10.1029/2018JD028320

Received 13 JAN 2018
Accepted 9 JUL 2018
Accepted article online 16 JUL 2018
Published online 3 AUG 2018

Abstract The development of BeiDou Navigation Satellite System (BDS) provides opportunities for real-time retrieval of precipitable water vapor (PWV), which is expected to significantly contribute to time-critical meteorological applications. In this study, observations from 17 stations of the Hong Kong Continuously Operating Reference Stations and 15 stations of the Crustal Movement Observation Network of China (CMONOC) are used to retrieve PWV based on the real-time precise point positioning ambiguity resolution approach. Real-time PWV products, retrieved from BDS observations of both summer (day of year 183–192) and winter (day of year 024–033) periods, are analyzed and validated using postprocessed Global Positioning System products. The results show that the real-time BDS PWV series agree well with the Global Positioning System PWV series. Root-mean-square values for the Hong Kong Continuously Operating Reference Stations and CMONOC stations are 2.0–3.5 and 2.5–4.0 mm, respectively. In addition, short initialization time, strong reliability, and good distribution could be achieved by applying the fixed solution instead of the float solution. With the gradual completion of BDS constellation, the BDS can independently contribute to real-time sensing of PWV and potentially contribute to time-critical meteorological applications.

1. Introduction

Atmospheric water vapor is essential for atmospheric energy transfer and formation of precipitation events. It plays an important role in various weather and climate processes. Numerous techniques have been used to measure the atmospheric water vapor, such as radiosonde (Coster, 1996; Niell et al., 2001) and water vapor radiometer (Gradinarsky & Elgered, 2000). The extraction of zenith tropospheric delay (ZTD) and precipitable water vapor (PWV) from Global Positioning System (GPS) observations, defined as GPS meteorology, was initially proposed by Bevis (1992). Extensive studies have been conducted for retrieving atmospheric parameters, and related data products are widely used in atmospheric research and applications. The accuracy of postprocessed GPS PWV can be as fine as 1.0 mm related to independent techniques, mostly radiosonde (Bock et al., 2016; Dousa, 2001; Karabatic et al., 2011; Niell et al., 2001; Van Baelen et al., 2005). However, some time-critical meteorological applications such as numerical weather prediction nowcasting and severe event monitoring require rapid updates of tropospheric results (Ding et al., 2017; Dousa & Vaclavovic, 2014; M. Li et al., 2015). The latency of real-time product is usually within a few minutes (Guerova et al., 2016), and the accuracy of the real-time PWV is better than 3 mm with respect to the meteorological sensors. Currently, real-time sensing of PWV has attracted much attention in the GPS meteorology community.

Since the International Global Navigation Satellite System Service (Dow et al., 2009) announced the availability of real-time precise satellite orbit/clock in 2012 (Caissy et al., 2012), interest in real-time precise point positioning (PPP) techniques has been significantly increasing. However, the performance of PPP-inferred atmospheric products is limited by the uncalibrated phase delay (UPD) (Ge et al., 2008), which lowers accuracy and leads to longer initialization time (Li et al., 2011; Liu et al., 2017; Shi & Gao, 2012). A root-mean-square (RMS) of about 1 mm in GPS PWV was obtained by ambiguity fixed PPP with respect to near-real-time products from the German Research Centre for Geosciences (GFZ) (Caissy et al., 2012; Gao et al., 2006), and the accuracy of real-time PPP-derived GPS PWV is better than 3 mm (Ahmed et al., 2016; Yuan et al., 2015). All these results demonstrated that the PPP technique can be implemented in the retrieval of accurate real-time PWV and time-critical applications.

As of July 2017, BeiDou Navigation Satellite System (BDS) consists of five Geostationary Earth Orbit, six Inclined Geosynchronous Orbit (IGSO), and three Medium Earth Orbiting satellites and it is expected to

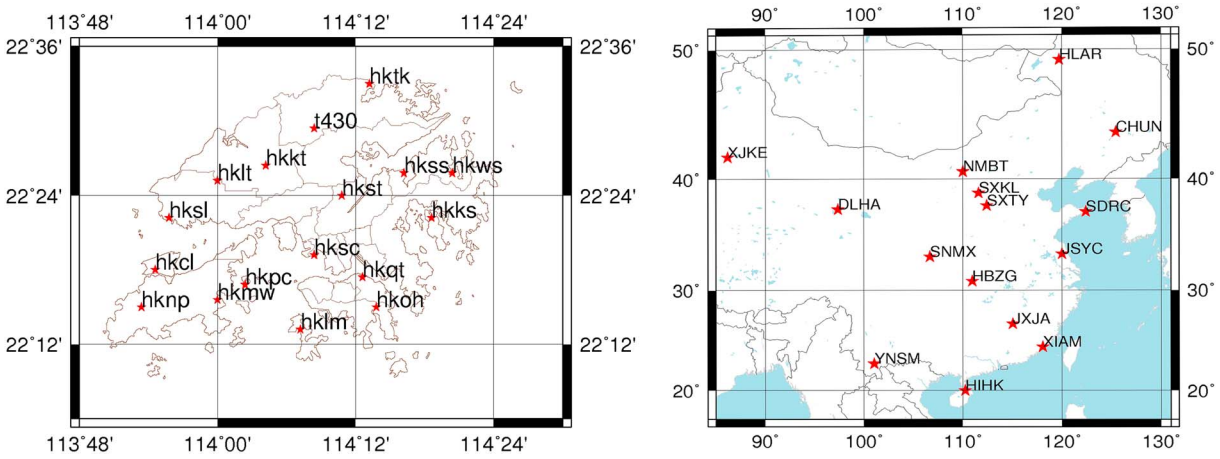

Figure 1. Distribution of selected stations in Hong Kong CORS (left) and CMONOC (right). CORS = Continuously Operating Reference Stations; CMONOC = Crustal Movement Observation Network of China.

be operated as a full constellation by the year 2020 (China Satellite Navigation Office, 2012). With the development of BDS, X. Li et al. (2015) demonstrated that the combination of BDS and GPS observations could make a better performance of PWV retrieval than a single system. However, as an independent satellite navigation system, BDS is expected to have the independent capability for meteorological applications without the help of other navigation systems. Meanwhile, the satellite constellation design of BDS is different from that of GPS. Therefore, it is important and valuable to investigate the performance of BDS only for PWV retrieval. X. Li et al. (2015) evaluated the performance of postprocessed BDS PWV, and an improved method of BDS PWV retrieval was demonstrated by Lu et al. (2017). But so far little work has been reported on the improvement of the real-time BDS PWV estimated with the PPP ambiguity resolution approach.

In this study, observations from 17 stations of the Hong Kong Continuously Operating Reference Stations (CORS) and 15 stations of the Crustal Movement Observation Network of China (CMONOC) were used to retrieve BDS PWV based on the real-time PPP ambiguity resolution approach. The initialization time, reliability, and accuracy were analyzed to evaluate the performance of real-time BDS PWV with respect to postprocessed GPS PWV. This article is organized as follows. Section 2 describes BDS data sets from Hong Kong and CMONOC networks and the BDS ZTD/PWV extraction with real-time PPP ambiguity resolution strategies. Next in section 3, the experiment and analysis are discussed in detail. Finally, the conclusions and perspectives are presented in section 4.

2. Data and Method

2.1. Tracking Network and Data Collection

The Hong Kong tracking network consists of 18 CORS, and the distance between two adjacent stations is approximately 10 to 15 km. The dense distribution of stations enables the provision of high-quality products for users in most areas. The CMONOC includes 2,260 stations, which is established to monitor crustal movement and gravity changes in China. These stations can provide high-quality observations covering the entirety of the Chinese mainland.

In this study, observations from 32 stations (17 in the Hong Kong CORS and 15 in CMONOC) were employed to retrieve the BDS PWV product. The distribution of these stations is shown in Figure 1. All selected stations can collect BDS and GPS observations simultaneously and continuously. The number of visible satellites (NSAT) and the Position Dilution of Precision of station HKMW (from Hong Kong CORS) and station JXJA (from CMONOC) on day of year (DOY) 024, 2016 are shown in Figure 2. These two stations are capable of tracking more than six BDS satellites simultaneously, which will contribute to a better geometry condition and more accurate PWV estimates for BDS.

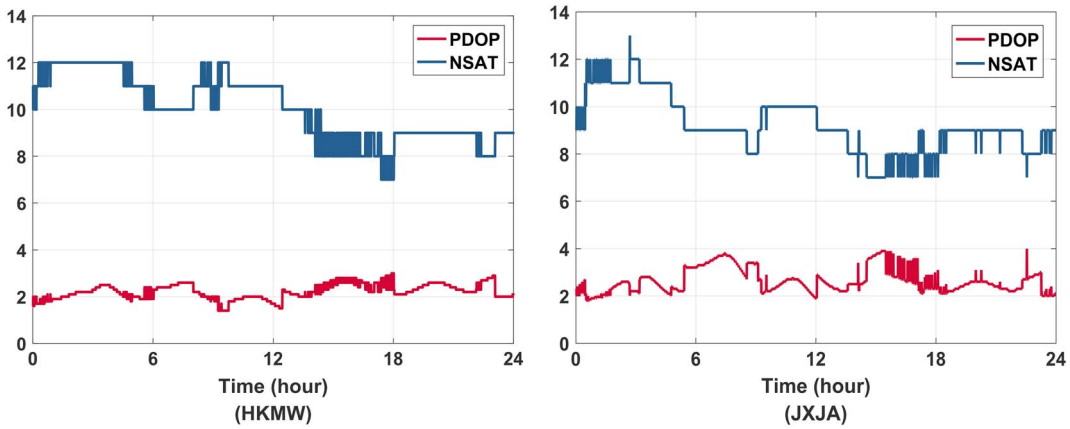

Figure 2. NSAT and PDOP at stations HKMW (Hong Kong CORS) and JXJA (CMONOC) on DOY 024, 2016. PDOP = Position Dilution of Precision; CORS = Continuously Operating Reference Stations; CMONOC = Crustal Movement Observation Network of China; DOY = day of year.

2.2. Real-Time BDS PWV Retrieval

The ionosphere-free (IF) combination of dual-frequency pseudorange and carrier phase is commonly applied in PPP processing to eliminate the effect of the ionosphere. The observation equation can be formulated as

$$\begin{aligned} P^s_{r,\mathrm{IF}} &= \rho^s_r g + c(t_r - t^s) + c\left(d_{r,\mathrm{IF}} - d^s_{\mathrm{IF}}\right) + T^s_r + e^s_{r,\mathrm{IF}} \\ L^s_{r,\mathrm{IF}} &= \rho^s_r g + c(t_r - t^s) + \lambda_{\mathrm{IF}}\left(N^s_{r,\mathrm{IF}} + b_{r,\mathrm{IF}} - b^s_{\mathrm{IF}}\right) + T^s_r + \varepsilon^s_{r,\mathrm{IF}} \end{aligned} \tag{1}$$

where $P^s_{r,\mathrm{IF}}$ and $L^s_{r,\mathrm{IF}}$ represent the IF observations for code and phase measurements (meters), respectively; c represents the velocity of light (meter per second); λ_{IF} refers to the wavelength of the IF phase observation (meters); $N^s_{r,\mathrm{IF}}$ is the integer ambiguity of IF combination; $d_{r,\ \mathrm{IF}}$ and d^s_{IF} denote the code hardware delays at receiver and satellite sides, while $b_{r,\ \mathrm{IF}}$ and b^s_{IF} are corresponding phase delays; $e^s_{r,\mathrm{IF}}$ and $\varepsilon^s_{r,\mathrm{IF}}$ are the sum of noise and multipath of code and phase IF combination observation; and $\rho^s_r g$ denotes the geometric distance from satellites to receivers. Tropospheric delay T^s_r, which is the main object of interest in this study, consists of hydrostatic and wet components, both of which can be expressed by their individual zenith delay, gradients, and mapping functions:

$$T^s_r = mf_h \cdot Z_h + mf_w \cdot Z_w + mf_w \cdot \cot(e) \cdot (G_{\mathrm{N}} \cdot \cos(a) + G_{\mathrm{E}} \cdot \sin(a)) \tag{2}$$

Here Z_h and Z_w denote zenith hydrostatic delays (ZHD) and zenith wet delays (ZWD) (meters); mf_h and mf_w represent the hydrostatic and wet mapping functions. In this study, the Global Mapping Function (Boehm et al., 2006) was adopted. G_{N} and G_{E} are the north and east gradients, e and a indicate elevation and azimuth angles, respectively. ZHD could be calculated with sufficient accuracy by empirical models—Saastamoinen model in this study (Saastamoinen, 1972). ZWD is influenced by various factors in the atmosphere, and thus, it has a high degree of spatiotemporal instability, which makes it difficult to achieve the required accuracy with model calculations. Therefore, ZWD is usually modeled as an unknown parameter and estimated in the PPP data processing.

The coordinates of stations are fixed as known values in the PPP data processing. With the precise clock and orbit corrected, the parameter vector X to be estimated in the traditional BDS PPP data processing can be described as

$$X = \left(t_r, Z_w, G_{\mathrm{N}}, G_{\mathrm{E}}, t_r\left(\widetilde{N}^s_r\right)^T\right) \tag{3}$$

where $\widetilde{N}^s_r$ represent float ambiguities. It usually takes a few hours to allow a BDS PPP to achieve centimeter-level accuracy. The corresponding BDS tropospheric PWV estimates also require such long initialization time.

In addition, the UPD decreases the accuracy of BDS PWV (Shi & Gao, 2012). To improve the accuracy of BDS tropospheric estimation and shorten the initialization time, a PPP ambiguity resolution described by Li and Zhang (2012) was applied in this study.

Ambiguities in the traditional standard PPP model lose their integer property because of UPDs at both receivers and satellites. Fortunately, the wide-lane (WL) UPD barely changes over several months (Gabor & Nerem, 1999), and the narrow-lane (NL) UPD is quite stable over a short time period of several tens of minutes (Ge et al., 2008), thus enabling UPD estimation. Once the WL and NL ambiguities are fixed, the IF combination ambiguity is fixed as well.

A network solution is used to estimate the WL and NL UPDs by means of a least squares adjustment, and the observation equation can be presented as follows:

$$\begin{bmatrix} R_1 \\ R_2 \\ \cdots \\ R_n \end{bmatrix} = \begin{bmatrix} C_1 & S_1 \\ C_2 & S_2 \\ \cdots & \cdots \\ C_n & S_n \end{bmatrix} \cdot \begin{bmatrix} d_r \\ d^s \end{bmatrix} \tag{4}$$

Assume that there are n stations tracking m satellites, where the matrix R indicates the matrices of ambiguity fractional parts for each satellite-station link; d_r and d^s denote the matrices of UPDs at receiver and satellite, respectively; C and S are the corresponding coefficient matrix of UPDs of receivers and satellites. To obtain stable WL UPD products, the BDS satellite-induced code bias should be corrected before the UPD estimation. For IGSO and Medium Earth Orbiting satellites, the code bias can be eliminated by a piecewise linear correction model proposed by Wanninger and Beer (2015), whereas for Geostationary Earth Orbit satellites, it can be corrected by sidereal wavelet filter. The precise BDS ambiguities estimated by multi-Global Navigation Satellite System PPP also provide an important premise to obtain high-precision NL UPDs. In addition, common errors between stations can be absorbed into satellite UPDs under the condition of a denser and small network, which leads more stable UPD products.

Real-time UPDs can be estimated epoch by epoch and then applied to the real-time ambiguity resolution. The Hatch-Melbourne-Wübbena combination is formulated here to obtain the WL ambiguity (Hatch, 1982; Melbourne, 1985; Wübbena, 1985). With the WL UPD corrected, the WL ambiguities will be fixed to integers by the round strategy (Dong & Bock, 1989). Then the NL ambiguities can be derived from the fixed WL ambiguities and IF combination ambiguities. With the NL UPD corrected, the integer NL ambiguity can be obtained by the LAMBDA method (Teunissen et al., 1999). After obtaining the integer ambiguities, the estimated parameter vector X can be shown as

$$X = (t_r, Z_w, G_N, G_E) \tag{5}$$

The sequential least squares method is adopted here for estimation of those parameters (Li et al., 2013). We estimated receiver clock offset t_r as a white noise process; both ZWD (Z_w) and the horizontal gradients (G_N, G_E) are modeled as random walk process, and the noise intensity of ZWD is set as 15 mm/$\sqrt{\text{hr}}$. A flowchart of the processing strategies for BDS real-time PWV extraction is presented in Figure 3, and the details are provided in Table 1.

With accurate ZWD estimates, the PWV can be obtained by

$$\text{PWV} = \Pi(T_m) \cdot Z_w \tag{6}$$

The parameter $\Pi(T_m)$ can be calculated by the atmospheric mean temperature T_m (Bevis, 1992):

$$\Pi(T_m) = \frac{10^6}{\rho_w R_v \left(\frac{k_3}{T_m} + k_2'\right)} \tag{7}$$

where R_v denotes the specific gas constant of PWV, which is generally 461.51 JK^{-1}/kg; ρ_w = 999.97 kg/m^3 denotes the density of liquid water; and $k_2' = 22.1 \pm 2.2$ (K/hpa) and $k_3 = 373900 \pm 1200$ (K^2/hpa) are atmospheric refraction coefficients. In later calculations of this study, they are all considered as constant

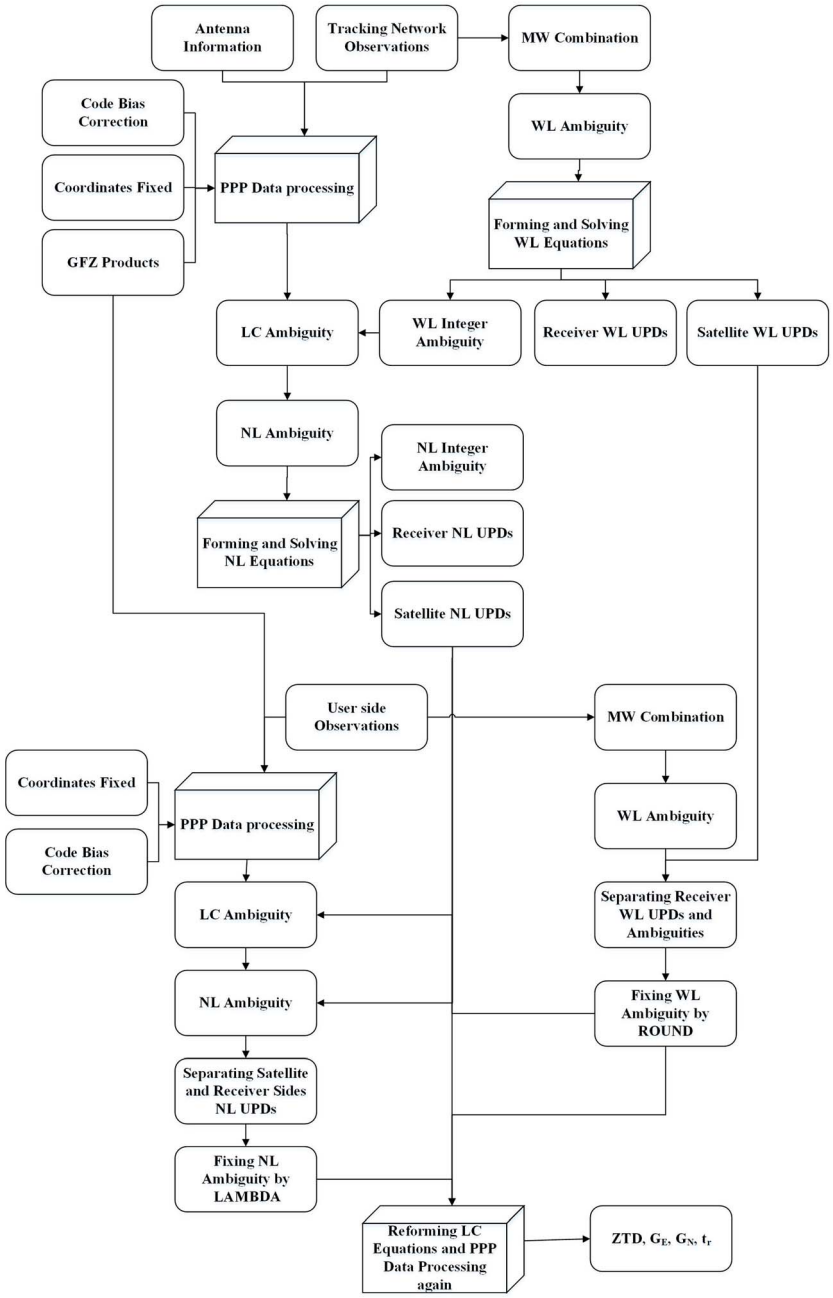

Figure 3. Strategy for real-time BDS ZTD/PWV extraction. BDS = BeiDou Navigation Satellite System; ZTD = zenith tropospheric delay; PWV = precipitable water vapor; PPP = precise point positioning; WL = wide lane; NL = narrow lane; UPDs = uncalibrated phase delays.

parameters $k_2^{'} = 22.1\ \ (\mathrm{K/hpa})$ and $k_3 = 373900\ \ (\mathrm{K^2/hpa})$. Because the difference between T_m from European Centre for Medium-Range Weather Forecasts (ECMWF) and from global radiosonde observations is less than 2 K for most stations (Wang et al., 2005), we use T_m from ECMWF reanalysis center to convert ZWD to PWV.

With the a priori ZHD and wet delay parameter, ZTD can be reconstructed. To retrieve the accurate ZWD from the PPP-derived ZTD, the more accurate ZHD is calculated by using pressure parameters from the ECMWF reanalysis. Then, ZWD is generated by the PPP-derived ZTD with the accurate ZHD estimations subtracted. Finally, ZWD could be converted into PWV following equation (6).

Table 1
PPP Processing Strategy for ZTD/PWV Estimation in Real-Time Mode

Model	Processing strategies
Estimator	Sequential least squares estimator
Observations	BDS observations from the Hong Kong CORS and CMONOC
Signals	B1/B2
Sampling rate	30 s
Elevation cutoff	7°
Weight for observations	Elevation-dependent weighting strategy
Satellite orbit	Corrected
Satellite clock	Corrected
Zenith tropospheric delay	Initial model + random walk model
Tropospheric gradients	Random walk model
Mapping function	Global Mapping Function (GMF)
Phase-windup effect	Corrected
Receiver clock	Estimated, white noise
Station displacement	Solid Earth tide, pole tide, ocean tide loadingIERS Convention 2010
Satellite antenna phase center	Corrected
Receiver antenna phase center	Corrected
Coordinates of stations	Fixed
Ambiguities	Undifferenced ambiguity resolution is applied

Note. ZTD = zenith tropospheric delay; PWV = precipitable water vapor; CORS = Continuously Operating Reference Stations; CMONOC = Crustal Movement Observation Network of China.

3. Results and Analysis

In this study, we processed BDS observations in real-time and tropospheric parameters were estimated every 30 s. The station coordinates were fixed to weekly solutions. Because International Global Navigation Satellite System Service tropospheric products were unavailable for Hong Kong CORS and the CMONOC stations, we employed the Positioning and Navigation Data Analyst software to generate the GPS tropospheric product by using the postprocessing network solution. It has an accuracy of less than 1 mm with respect to radiosonde (Dousa, 2001; Niell et al., 2001). Thus, the postprocessed GPS PWV can be used as standard reference, and the initialization time, reliability, and accuracy were selected as indicators to validate the performance of the real-time BDS PWV product.

3.1. Initialization Time of Real-Time BDS PWV

The initialization process is completed once differences between the estimated troposphere results and reference products are maintained lower than a given value. In this study, a value of 3 mm (about 20 mm in ZTD) was set, which is a common threshold for the implementation of PWV in meteorological applications (Offiler, 2010). Figure 4 shows the real-time BDS PWV series of two stations: HKKS from Hong Kong CORS and

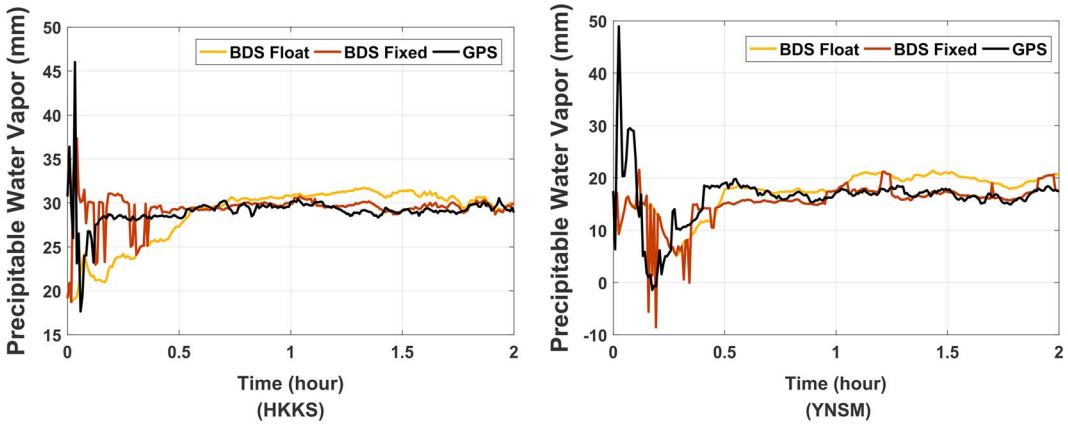

Figure 4. Real-time BDS PWV series derived from float (yellow line) and fixed (brown line) solutions, and GPS PWV series (black line) at station HKKS (left) and YNSM (right) for the first 2 hr of DOY 024, 2016. BDS = BeiDou Navigation Satellite System; PWV = precipitable water vapor; GPS = Global Positioning System; DOY = day of year.

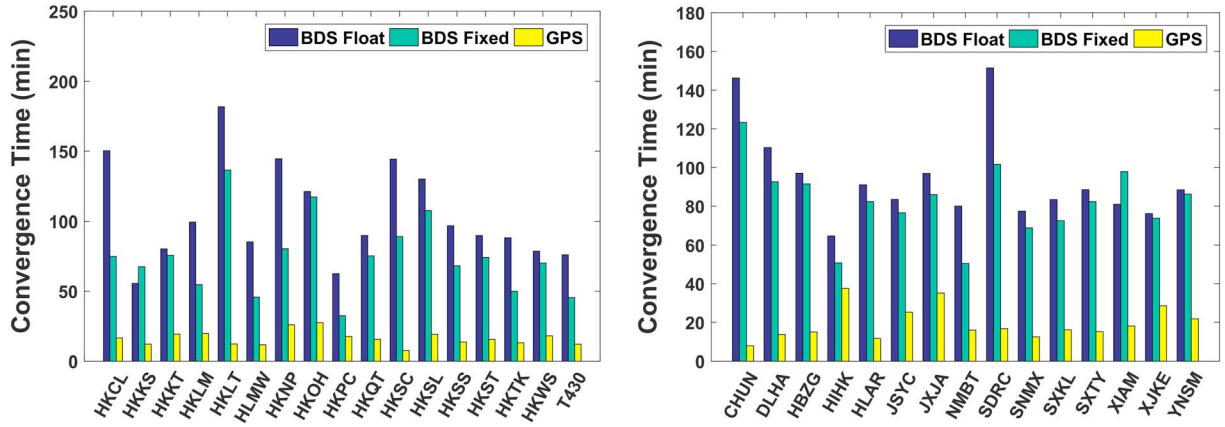

Figure 5. Average initialization time of real-time PWV derived from BDS and GPS observations during DOY 024–032, 2016. BDS = BeiDou Navigation Satellite System; PWV = precipitable water vapor; GPS = Global Positioning System; DOY = day of year.

YNSM from CMONOC. The yellow and brown curves indicate the real-time BDS PWV retrieved from the float and fixed solutions, respectively, whereas the black curves refer to the GPS PWV series. The figure shows initialization procedures for the three solutions. As expected, the fixed solution required a shorter initialization time than the float solution after the ambiguities were fixed to correct integers (Liu et al., 2017).

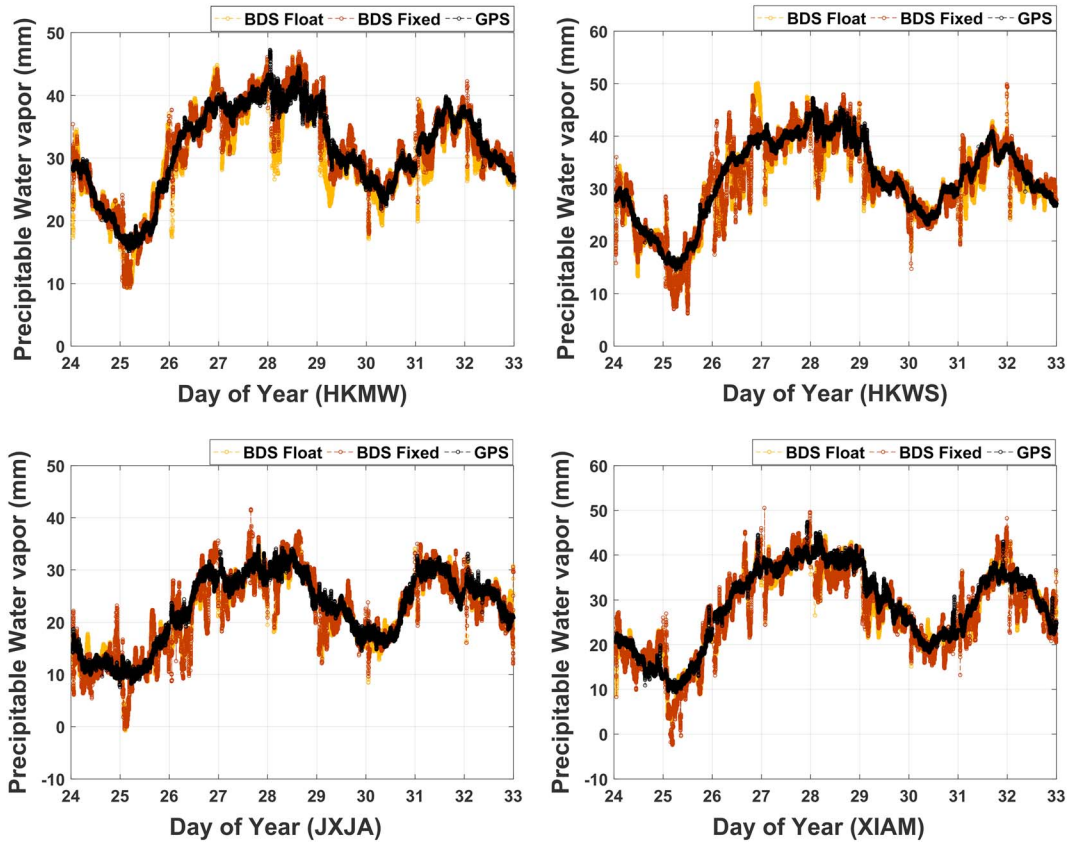

Figure 6. Real-time PWV derived from BDS PPP solution (float: yellow line; fixed: brown line) and postprocessed PWV from GPS PPP (black line) at two stations (HKMW and HKWS) of Hong Kong CORS (top row) and two stations (JXJA and XIAM) of CMONOC (bottom row). BDS = BeiDou Navigation Satellite System; GPS = Global Positioning System; PPP = precise point positioning; CORS = Continuously Operating Reference Stations; CMONOC = Crustal Movement Observation Network of China.

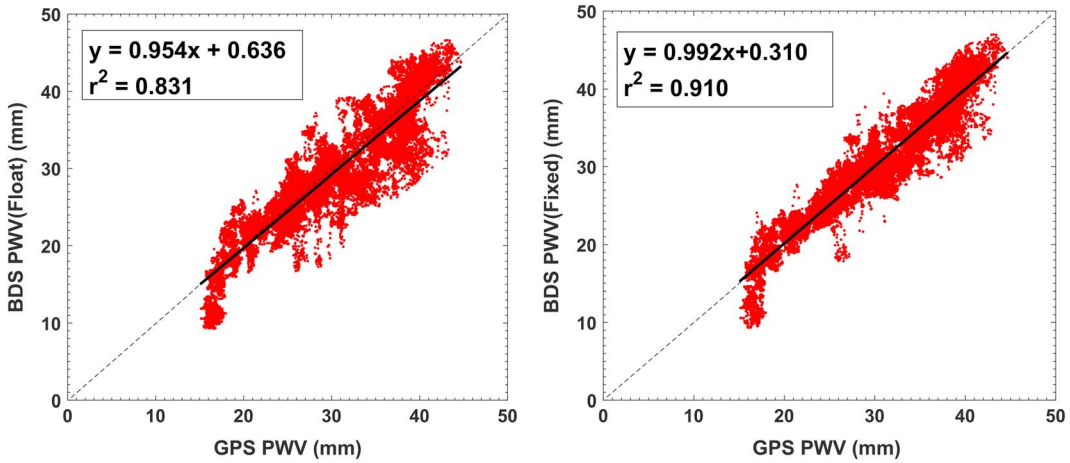

Figure 7. Correlation of PWV between real-time BDS solutions (float: left panel; fixed: right panel) and postprocessed GPS solution at station HKMW of the Hong Kong CORS. PWV = precipitable water vapor; BDS = BeiDou Navigation Satellite System; GPS = Global Positioning System; CORS = Continuously Operating Reference Stations.

We summarized the average initialization time, and the results are shown in Figure 5. The blue/green columns indicate the real-time BDS PWV with the float/fixed solutions and the yellow columns represent GPS PWV. BDS float solution required the longest initialization time, and the real-time BDS PWV derived from PPP fixed solution consumed a shorter time for the convergence process for all stations, but it was still much longer than that required by GPS. The average initialization time of BDS PWV with the float solution were 104.4 and 94.4 min for Hong Kong and CMONOC stations, respectively, which could be shortened to 74.4 and 82.5 min for the BDS PWV with the fixed solution. Compared with GPS, the convergence process for BDS was much longer, which may be due to the slow movement of GEO and IGSO satellites (Lu et al., 2015).

3.2. Correlation Between BDS PWV and GPS PWV

To verify the reliability of the results, a correlation analysis was performed. Figure 6 shows the PWV series of stations HKMW and HKWS from the Hong Kong CORS and JXJA and XIAM from CMONOC. The yellow and brown lines indicate real-time BDS PWV with the float/fixed solutions, whereas the black line refers to postprocessed GPS PWV products. In our real-time processing, the PPP estimator was reset every single day, and thus, an obvious initialization time can be found for the first few hours of each day. The real-time BDS PWV agreed well with the postprocessed GPS PWV. Compared with the reference data, the real-time BDS PWV series with the fixed solution was more accurate and reliable than that with the traditional float solution. In addition, the real-time BDS PWV product with the fixed solution exhibited less outliers and was not susceptible to noise.

Figure 7 presents the linear correlation between the real-time BDS PWV and postprocessed GPS PWV for station HKMW on DOY 024–033 of 2016. The BDS PWV estimated with the float and fixed solutions is shown in the left and right panels, respectively. A strong correlation was found between real-time BDS PWV and postprocessed GPS PWV. The correlation coefficient between BDS PWV with fixed solution and GPS PWV was 0.95 at station HKMW, which shows high relevance with the GPS product. The statistical results are summarized in Table 2, showing that the BDS PWV product with the fixed solution showed a smaller deviation from the GPS

Table 2
Mean Bias Between BDS and GPS

	Hong Kong (DOY 183–192)	Hong Kong (DOY 024–033)	CMONOC (DOY 024–033)
C(Float)-G	−1.37	−0.871	−0.932
C(Fixed)-G	−0.15	−0.337	−0.719

Note. All values in millimeter. BDS = BeiDou Navigation Satellite System; GPS = Global Positioning System; DOY = day of year.

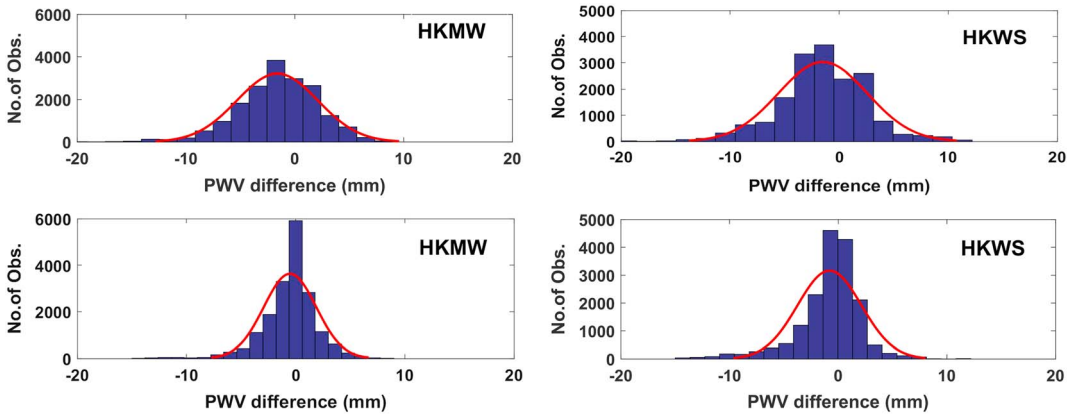

Figure 8. Distribution of differences in PWV between real-time BDS solutions (float: top row; fixed: bottom row) and postprocessed GPS solutions at stations HKMW (left) and HKWS (right). PWV = precipitable water vapor; BDS = BeiDou Navigation Satellite System; GPS = Global Positioning System.

product than float solution. To further investigate the sensitivity of the two processing solutions, we analyzed the experimental results of the Hong Kong CORS in two different periods. The statistics show that the BDS PWV product with the fixed solution was improved with smaller mean bias compared with that of the float solution in both summer (DOY 183–192, 2016) and winter (DOY 024–033, 2016).

3.3. Accuracy of Real-Time BDS PWV

The distribution of differences in PWV between real-time BDS solutions and GPS postprocessed solution at stations HKMW (left) and HKWS (right) of the Hong Kong CORS is presented in Figure 8. Frequency counts of PWV differences between the BDS fixed solution in real-time mode and GPS postprocessed solution were closer to the normal distribution than those with the float solutions. RMS values of the PWV differences were 2.32 mm for station HKMW and 2.86 mm for station HKWS. Compared with the float solution (3.98 mm for station HKMW and 4.22 mm for station HKWS), the improvement was approximately 41.5% and 32.2%. In addition, standard deviation (STD) values and mean biases for the two stations were 2.28 and −0.47 mm (HKMW), and 2.77 and −0.722 mm (HKWS), respectively.

Figure 9 shows the distribution of PWV differences between BDS real-time PPP solutions and GPS postprocessed solution at JXJA and XIAM of CMONOC. As expected, the frequency distribution of PWV differences between real-time BDS with the fixed solution and postprocessed GPS was closer to the normal distribution than those retrieved from the float solution. RMS values of PWV estimated with the float solution were 3.49

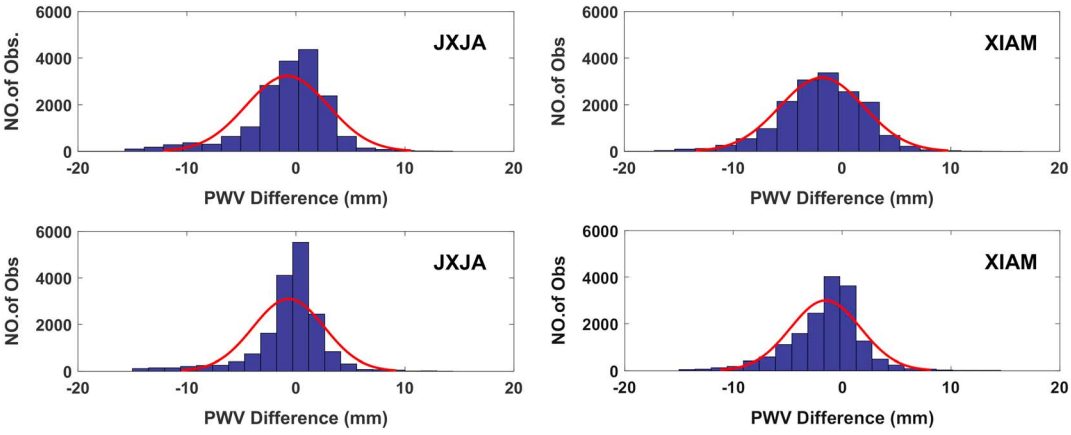

Figure 9. Distribution of differences in PWV between real-time BDS solutions (float: top row; fixed: bottom row) and postprocessed GPS solution at stations JXJA (left) and XIAM (right). PWV = precipitable water vapor; BDS = BeiDou Navigation Satellite System; GPS = Global Positioning System.

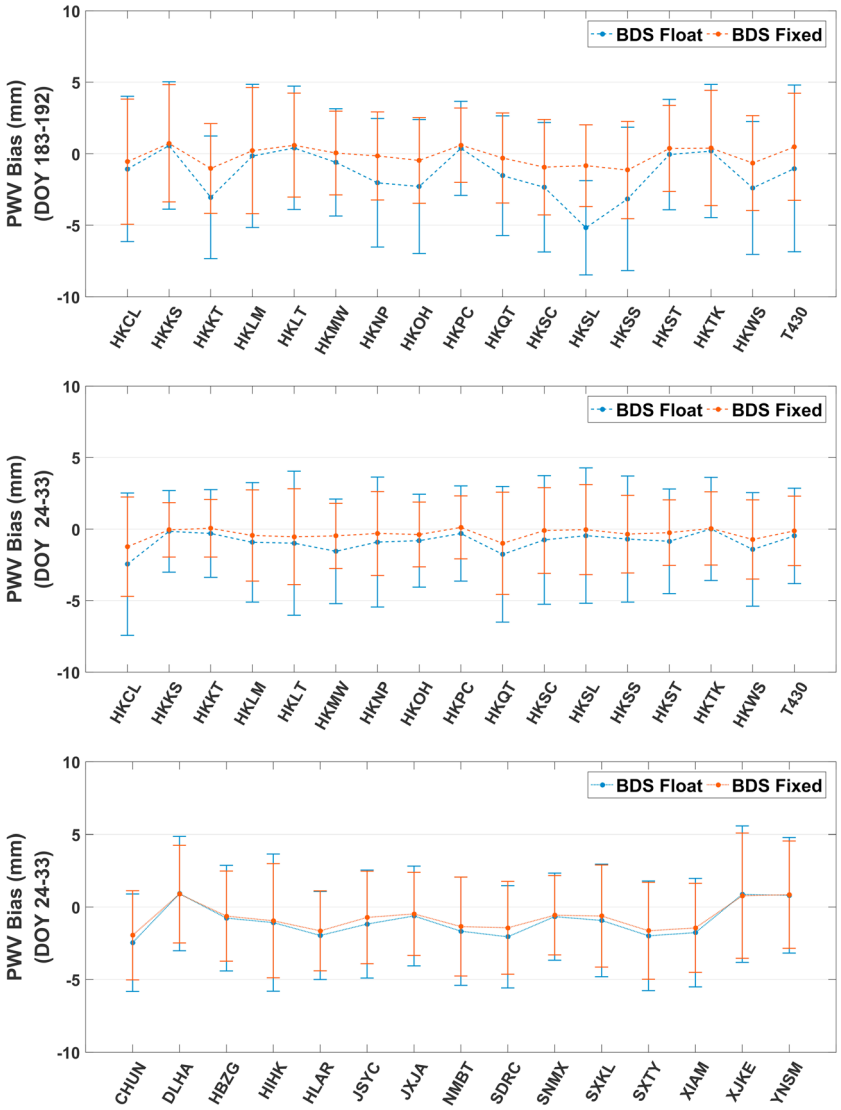

Figure 10. Accuracy of real-time BDS PWV derived from float/fixed solutions in Hong Kong CORS and CMONOC. PWV = precipitable water vapor; BDS = BeiDou Navigation Satellite System; DOY = day of year; CORS = Continuously Operating Reference Stations; CMONOC = Crustal Movement Observation Network of China.

and 4.14 mm at stations JXJA and XIAM, and they could be improved to 2.90 and 3.39 mm with the fixed solution. The accuracy of the real-time BDS PWV with the fixed solution could be improved by 16.9% and 18.1% for the two stations. Furthermore, STD at station JXJA was reduced from 3.44 to 2.86 mm, whereas it was reduced from 3.74 to 3.07 mm at station XIAM. The mean bias between the real-time BDS PWV and postprocessed GPS PWV also declined from −0.618 mm to −0.474 mm (JXJA) and − 1.77 mm to −1.44 mm (XIAM), respectively, after applying the fixed solution.

Figure 10 plots the mean bias and STD of all stations with respect to the postprocessed GPS PWV product. For a sensitivity test, experimental results for the Hong Kong stations during two different periods were analyzed. The average STD values were 2.72 and 3.42 mm for the Hong Kong stations during DOY 024–033 (top panel) and DOY 183–192 (middle panel), with improvements of 32.1% and 22.5% from that of the float BDS PWV. The mean bias was also reduced from 0.87 mm to −0.34 mm and − 1.37 mm to −0.15 mm during the two seasons. The average STD values for all stations were 2.85 and 3.31 mm for the Hong Kong and CMONOC stations. This suggests that the accuracy of BDS PWV can be improved significantly, especially in the Hong Kong areas, by applying the fixed solution. The greater improvement for the Hong Kong CORS may be attributed to the more stable and accurate UPD products derived from the smaller network.

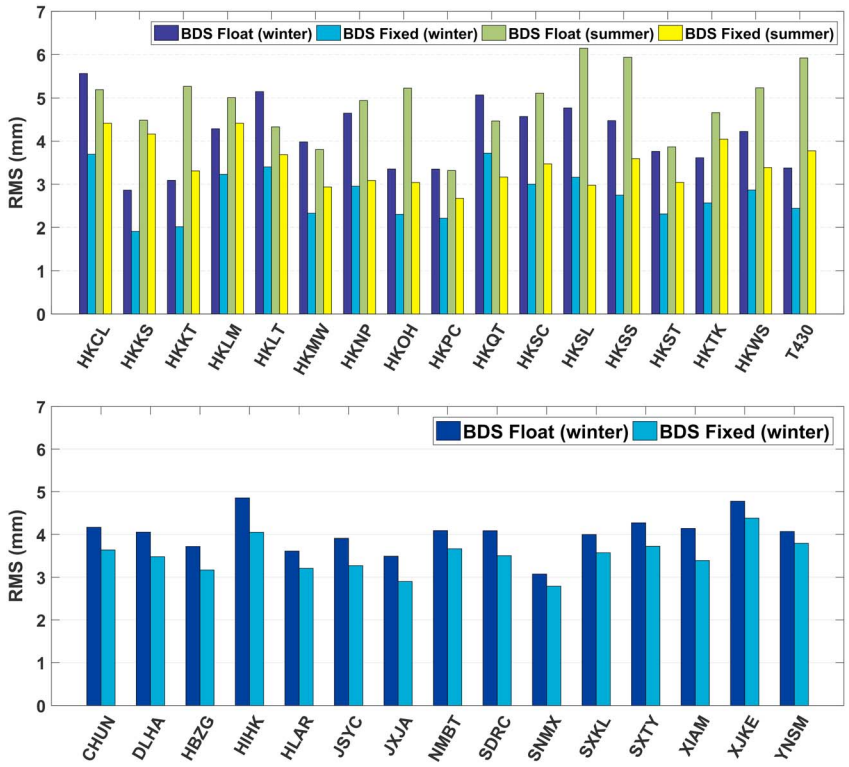

Figure 11. RMS of real-time BDS PWV with float/fixed solutions in the Hong Kong CORS (top) and CMONOC (bottom). RMS = root-mean-square; PWV = precipitable water vapor; BDS = BeiDou Navigation Satellite System; CORS = Continuously Operating Reference Stations; CMONOC = Crustal Movement Observation Network of China.

The average RMS values of differences in PWV for all stations in the Hong Kong CORS and CMONOC are also summarized in Figure 11. The top panel of Figure 11 represents the average RMS values for the Hong Kong stations during summer (DOY 183–192) and winter (DOY 024–033), whereas the bottom panel denotes CMONOC winter results during DOY 024–033, 2016. Compared with products obtained by the float solution, the accuracy of BDS-derived PWV with the fixed solution was higher. The average RMS values of the Hong Kong stations were 2.76 mm in winter and 3.28 mm in summer. Compared with the traditional float solution, the results demonstrate that the BDS PWV products improved by 33.2% and 27.5% during summer and winter after applying the fixed solution. The average RMS values were 3.12 mm for the Hong Kong stations and 3.50 mm for CMONOC stations. The accuracy of the real-time BDS PWV with the fixed solution was improved by approximately 30.4% for the Hong Kong CORS and 12.8% for CMONOC. Higher accuracy could be clearly achieved for the real-time BDS PWV with the fixed solution than the product with the float solution. In addition, the improvement of the PWV accuracy was more significant for the Hong Kong CORS than for CMONOC.

4. Conclusions

In this study, 32 stations (17 in the Hong Kong CORS and 15 in CMONOC) were used to retrieve BDS PWV products based on the real-time PPP ambiguity resolution approach. We conducted a detailed analysis of factors, including initialization time, reliability, and the accuracy of the real-time BDS PWV product.

As for the convergence, average initialization times of 104.4 and 94.4 min are required by the traditional float BDS PWV product for the Hong Kong CORS and CMONOC network. By applying the fixed solution, the average initialization time could be shortened to 74.4 and 82.5 min, with improvements of 27.1% and 11.6%, respectively. In the correlation analysis, the real-time BDS PWV agreed well with the GPS products. The fixed real-time BDS PWV was more accurate and reliable than those of the float solution. Furthermore, mean biases between BDS PWV and GPS PWV were close to zero. The comparative experiment results showed that the fixed BDS PWV product has a similar improved performance during both summer and winter.

Differences in distribution, STD, and RMS values were used as indicators to determine the accuracy of the real-time BDS PWV. The distribution of differences in the BDS fixed solution was close to the normal distribution. RMS values of the fixed solution were 1.91–4.42 and 2.79–4.38 mm, for the Hong Kong CORS and CMONOC, respectively. The accuracy was improved by 30.4% for the Hong Kong CORS and 12.8% for CMONOC from the product with the float solution. The greater improvement for the Hong Kong CORS may be attributed to the more stable and accurate UPD products derived from the smaller network.

The results reveal that the BDS and ambiguity resolution are effective in real-time meteorological applications, although the real-time BDS PWV product still requires a long initialization time. The performance of BDS could be further improved with the completion of the constellation by the year 2020.

Acknowledgments
We acknowledge IGS, MGEX, and BETN for providing the GPS and BDS data. The data are available at ftp://cddis.gsfc.nasa.gov/gnss/data/campaign/mgex/. Thanks also go to the PANDA software provided by GFZ.

References

Ahmed, F., Teferle, F. N., Bingley, R., & Laurichesse, D. (2016). Comparative analysis of real-time precise point positioning zenith total delay estimates. *GPS Solutions*, *20*(2), 187–199. https://doi.org/10.1007/s10291-014-0427-z

Bevis, M. (1992). GPS meteorology: Remote sensing of atmospheric water vapor using GPS. *Journal of Geophysical Research*, *97*(D14), 15,787–15,801. https://doi.org/10.1029/92JD01517

Bock, O., Bosser, P., Pacione, R., Nuret, M., Fourrié, N., & Parracho, A. (2016). A high-quality reprocessed ground-based GPS dataset for atmospheric process studies, radiosonde and model evaluation, and reanalysis of HyMex special observing period. *Quarterly Journal of the Royal Meteorological Society*, *142*(S1), 56–71. https://doi.org/10.1002/qj.2701

Boehm, J., Niell, A., Tregoning, P., & Schuh, H. (2006). Global Mapping Function (GMF): A new empirical mapping function based on numerical weather model data. *Geophysical Research Letters, 33*, L07304. https://doi.org/10.1029/2005GL025546

Caissy, M., Agrotis, L., Weber, G., Hernandez-Pajares, M., & Hugentobler, U. (2012). Coming soon: The international GNSS real-time service. *GPS World*.

China Satellite Navigation Office (2012). BeiDou navigation satellite system signal in space interface control document. http://gge.unb.ca/test/beidou_icd_english.pdf

Coster, A. J. (1996). Measurements of precipitable water vapor by GPS, radiosondes, and a microwave water vapor radiometer. In *Proceedings of ION GPS-97, Institute of Navigation* (Vol. 1996, pp. 625–634).

Ding, W., Teferle, F. N., Kazmierski, K., Laurichesse, D., & Yuan, Y. (2017). An evaluation of real-time troposphere estimation based on GNSS precise point positioning. *Journal of Geophysical Research: Atmospheres*, *122*, 2779–2790. https://doi.org/10.1002/2016JD025727

Dong, D. N., & Bock, Y. (1989). Global positioning system network analysis with phase ambiguity resolution applied to crustal deformation studies in California. *Journal of Geophysical Research*, *94*(B4), 3949–3966. https://doi.org/10.1029/JB094iB04p03949

Dousa, J. (2001). Towards an operational near real-time precipitable water vapor estimation. *Physics & Chemistry of the Earth Part A Solid Earth & Geodesy*, *26*(3), 189–194. https://doi.org/10.1016/S1464-1895(01)00045-X

Dousa, J., & Vaclavovic, P. (2014). Real-time zenith tropospheric delays in support of numerical weather prediction applications. *Advances in Space Research*, *53*(9), 1347–1358. https://doi.org/10.1016/j.asr.2014.02.021

Dow, J. M., Neilan, R. E., & Rizos, C. (2009). The international GNSS service in a changing landscape of global navigation satellite systems. *Journal of Geodesy*, *83*(3–4), 191–198. https://doi.org/10.1007/s00190-008-0300-3

Gabor, M. J., & Nerem, R. S. (1999). GPS carrier phase ambiguity resolution using satellite-satellite single difference. In *Proceedings of 12th international technical meeting of the satellite division of the U.S. Institute Navigation GPS 99* (pp. 14–17). USA: September, Nashville, TN.

Gao, Y., Zhang, Y., & Chen, K. (2006). Development of a real-time single-frequency precise point positioning system and test results. In: *Proceedings of Ion GNSS,* 2297–2303, 26–29 September, Fort Worth.

Ge, M., Gendt, G., Rothacher, M., Shi, C., & Liu, J. (2008). Resolution of GPS carrier-phase ambiguities in precise point positioning (PPP) with daily observations. *Journal of Geodesy*, *82*(7), 389–399. https://doi.org/10.1007/s00190-007-0187-4

Gradinarsky, L. P., & Elgered, G. (2000). Horizontal gradients in the wet path delay derived from four years of microwave radiometer data. *Geophysical Research Letters*, *27*(16), 2521–2524. https://doi.org/10.1029/2000GL011427

Guerova, G., Jones, J., Dousa, J., Dick, G., Haan, S. D., Pottiaux, E., et al. (2016). Review of the state-of-the-art and future prospects of the ground-based GNSS meteorology in Europe. *Atmospheric Measurement Techniques*, *9*(11), 1–34.

Hatch, R. R. (1982). The synergism of GPS code and carrier measurements. In *International geodetic symposium on satellite Doppler positioning* (Vol. 1, pp. 1213–1231). International Geodetic Symposium on Satellite Doppler Positioning.

Karabatic, A., Weber, R., & Haiden, T. (2011). Near real-time estimation of tropospheric water vapour content from ground based GNSS data and its potential contribution to weather now-casting in Austria. *Advances in Space Research*, *47*(10), 1691–1703. https://doi.org/10.1016/j.asr.2010.10.028

Li, M., Li, W., Shi, C., Zhao, Q., Su, X., Qu, L., et al. (2015). Assessment of precipitable water vapor derived from ground-based BeiDou observations with precise point positioning approach. *Advances in Space Research*, *55*(1), 150–162. https://doi.org/10.1016/j.asr.2014.10.010

Li, X., Ge, M., Zhang, H., & Wickert, J. (2013). A method for improving uncalibrated phase delay estimation and ambiguity-fixing in real-time precise point positioning. *Journal of Geodesy*, *87*(5), 405–416. https://doi.org/10.1007/s00190-013-0611-x

Li, X., & Zhang, X. (2012). Improving the estimation of uncalibrated fractional phase offsets for PPP ambiguity resolution. *Journal of Navigation*, *65*(3), 513–529.

Li, X., Zhang, X., & Ge, M. (2011). Regional reference network augmented precise point positioning for instantaneous ambiguity resolution. *Journal of Geodesy*, *85*(3), 151–158. https://doi.org/10.1007/s00190-010-0424-0

Li, X., Zus, F., Lu, C., Dick, G., Ning, T., Ge, M., et al. (2015). Retrieving of atmospheric parameters from multi-GNSS in real time: Validation with water vapor radiometer and numerical weather model. *Journal of Geophysical Research: Atmospheres*, *120*, 7189–7204. https://doi.org/10.1002/2015JD023454

Liu, Y., Ye, S., Song, W., Lou, Y., & Chen, D. (2017). Integrating GPS and BDS to shorten the initialization time for ambiguity-fixed PPP. *GPS Solutions*, *21*(2), 333–343. https://doi.org/10.1007/s10291-016-0525-1

Lu, C., Li, X., Nilsson, T., Ning, T., Heinkelmann, R., Ge, M., et al. (2015). Real-time retrieval of precipitable water vapor from GPS and BeiDou observations. *Journal of Geodesy*, *89*(9), 843–856. https://doi.org/10.1007/s00190-015-0818-0

Lu, C., Li, X., Zus, F., Heinkelmann, R., Dick, G., Ge, M., et al. (2017). Improving BeiDou real-time precise point positioning with numerical weather models. *Journal of Geodesy*, *91*(9), 1–11.

Melbourne, W. G. (1985). The case for ranging in GPS-based geodetic systems. Paper presented at the first international symposium on precise positioning with the global positioning system, Rockville, MD, USA.

Niell, A. E., Coster, A. J., Solheim, F. S., Mendes, V. B., Toor, P. C., Langley, R. B., et al. (2001). Comparison of measurements of atmospheric wet delay by radiosonde, water vapor radiometer, GPS, and VLBI. *Journal of Atmospheric & Oceanic Technology*, *18*(6), 830–850. https://doi.org/10.1175/1520-0426(2001)018<0830:COMOAW>2.0.CO;2

Offiler, D. (2010). Product requirements document version 1.0—21 December 2010, EIG EUMETNET GNSS Water Vapour Programme (EGVAP-II).

Saastamoinen, J. (1972). Contributions to the theory of atmospheric refraction. *Bulletin Géodésique* (1946–1975), *105*(1), 279–298. https://doi.org/10.1007/BF02521844

Shi, J., & Gao, Y. (2012). Improvement of PPP-inferred tropospheric estimates by integer ambiguity resolution. *Advances in Space Research*, *50*(10), 1374–1382. https://doi.org/10.1016/j.asr.2012.06.036

Teunissen, P. J. G., Joosten, P., & Tiberius, C. C. J. M. (1999). Geometry-free ambiguity success rates in case of partial fixing. Proceedings of the National Technical Meeting of the Institute of Navigation, 201–207.

Van Baelen, J., Aubagnac, J. P., & Dabas, A. (2005). Comparison of near real time estimates of integrated water vapor derived with GPS, radiosondes, and microwave radiometer. *Journal of Atmospheric & Oceanic Technology*, *22*(2), 201–210. https://doi.org/10.1175/JTECH-1697.1

Wang, J., Zhang, L., & Dai, A. (2005). Global estimates of water-vapor-weighted mean temperature of the atmosphere for GPS applications. *Journal of Geophysical Research*, *110*, D21101. https://doi.org/10.1007/BF02522083

Wanninger, L., & Beer, S. (2015). BeiDou satellite-induced code pseudorange variations: Diagnosis and therapy. *Springer-Verlag New York, Inc*, *19*(4), 639–648.

Wübbena G. (1985). Software developments for geodetic positioning with GPS using TI-4100 code and carrier measurements. Paper presented at the first international symposium on precise positioning with the Global Positioning System, Rockville, MD, USA.

Yuan, Y., Zhang, K., Rohm, W., Choy, S., Norman, R., & Wang, C. (2015). Real-time retrieval of precipitable water vapor from GPS precise point positioning. *Journal of Geophysical Research: Atmospheres*, *119*, 10,044–10,057.